2021 4th International Symposium on Traffic Transportation and Civil Architecture (ISTTCA)

Finite Element Optimization Analysis of CFRP Reinforced box girder bridge Under Traffic Load

Xiangyu Li
School of Traffic and Transportation
Beijing Jiaotong University
Haidian District, Beijing 100044, China
18221163@bjtu.edu.cn

***Abstract*—In order to study the optimized influence of different pasting methods of CFRP on bridges, the ABAQUS finite element software was proposed, and combined with the structural form of Guangxi Nadezhong Bridge, the influence laws of CFRP pasting directions and CFRP pasting layers on the stress and deflection of bridges were discussed comprehensively. The results showed that the CFRP adhesion effectively reduced the structure stress, span deflection and cracking loads. And increasing pasting angle would decrease the reinforcement efficiency of CFRP, among which the pasting angles of 0° and 90° achieved the best reinforcement effect, reducing the structural stress and mid-span deflection by 17.6% and 17.3%, respectively, and increasing the cracking and flexural load by 3.5% and 5.3%, respectively. A larger number of CFRP layers would lead to gradual reduction of stress and mid-span deflection, and increasing cracking load. Accordingly, longitudinal and transverse CFRP application method and increasing the number of longitudinal CFRP fabric layers were recommended to optimize the bridge bearing structure.**

Keywords-CFRP reinforcement; finite element analysis; parametric analysis; reinforcement effect

I. INTRODUCTION

In recent years, with the increase of China's economic volume, the development and construction of highway bridges has also entered the new stage, and the scale of various bridges under construction and built has continuously set new world records. According to relevant data from the Ministry of Transport, by the end of 2017, there were 832,500 highway bridges in China. At present, more than half of the world's top ten cross-sea bridges, cable-stayed bridges, suspension bridges, etc., are located in China. At the same time, relevant specifications for vehicle load levels have been upgraded. And bridges in service not only are affected by bridge vehicle loads, but also suffer from material deterioration with increasing service life. Traditional bridge structure reinforcement methods include the increased section reinforcement method, prestressing reinforcement method, paste steel plate reinforcement method, shotcrete reinforcement method, etc. [1]. While the fiber reinforced material (CFRP) reinforcement method with light weight, high strength and high efficiency, corrosion resistance, fatigue resistance, easy construction and other characteristics has become one of the most common methods for bridge maintenance and reinforcement.

Fiber reinforced polymer (FRP) is one kind of composite material, common FRP materials include carbon fiber reinforced plastic (CFRP), glass fiber reinforced plastic (GFRP), aramid fiber reinforced plastic (AFRP) and basalt fiber reinforced plastic (BFRP), etc. Among them, due to the extremely high modulus of elasticity (over 180 GPa) and tensile strength (over 1300 MPa), and the advantages of corrosion resistance properties, environmental durability and inherent tailorability, the CFRP is widely used not only for the rehabilitation of existing buildings, but also the infrastructure reinforcement and the construction of new facilities [2-4].

Applications of CFRP materials include retrofitting of reinforced and unreinforced masonry walls, seismic retrofitting of bridges and buildings, repair and strengthening of concrete structures, metal and wood beams, and restoration of historic sites, offshore platforms and unique structures such as chimneys [5-7].The research results have shown that when loading the beams reinforced with pasting carbon fiber, the crack development is effectively controlled, and the stress performance of the beams has significantly improved, the reinforced beams can meet all mechanical indexes. In recent years, the construction industry has become one of the largest consumers of CFRP worldwide [8-12]. As concrete infrastructures are designed to serve different users for decades, the CFRP is required to meet different load demands [13-15]. Consequently, researchers begin to explore the performance of CFRP reinforcement systems under various load types such as static action, seismic action, fatigue action, impact, explosion, and fire. promoting the development of CFRP with greater performance and wider applications range [16-19]. And new CFRP materials including jet CFRP [20] and refractory CFRP [21] have also been investigated recently. Based on the CFRP researches, American Concrete Institute (ACI) published the first design guide for CFRP, ACI 440.1R-01.

Existing literature about structure strengthening of CFRP are extensive, including axial compression, flexural and shear tests and finite element analysis, and corresponding computational methods have also been proposed.

However, most of the above studies are at the laboratory stage, projects strengthened with CFRP especially large span bridges in engineering are still needed in research. The small and medium-span bridges account for a relatively large amount in foundation construction, while the researches about them are quite insufficient. Once structural damage occurs, CFRP is the easiest way for strengthening. Accordingly, conducting CFRP reinforcement researches on bridges in service is necessary.

978-1-6654-2592-6/21/$31.00 ©2021 IEEE

Considering the cost of actual strengthening with CFRP, the ABAQUS software was adopted to propose the finite element model to simulate and analyze the service bridges under traffic loads in this thesis. Through reinforcing bridges with CFRP, taking the stress and deflection variation as the test indexes, the influence of parameters including CFRP adhesion directions and layer numbers on reinforced bridges in service were explored. Besides, the cracking load was further explored, providing a reference for the research of engineering reinforcement.

II. PROJECT OVERVIEW

Located in Guangxi Province, the Nadezhong bridge is a three-span prestressed concrete simple-supported multi-box girder bridge, span combination of 5m + 3 × 20m + 5m, the total length of 70m, width 11.5m, with columnar pier. The bridge deck and piers are made of C50 concrete, with the density of 2600kg/m3, and elasticity modulus E=3.45×104MPa. The reinforcement elasticity modulus Es=1.95×105MPa.The CFRP adhesion angle and layer number are regarded as the model variables, and the specific parameters are shown in Table 1. The diagram of CFRP pasting angles are shown in Fig.1.

TABLE I. MODEL PARAMETERS

Model number	CFRP Pasting angle	Number of layers	Maximum stress in span /MPa	Maximum deflection in the span /mm	Remarks
B-1	-	-	3.4	4.6	Model comparison
BC-1	0°	1	3.1	4.3	Pasting angle comparison
BC-2	30°		3.1	4.3	
BC-3	45°		3.2	4.3	
BC-4	60°		3.2	4.4	
BC-5	90°	1	3.3	4.5	
BC-6	0°+90°	1	2.8	3.8	
BC-7	90°	2	3.2	4.4	Layer number comparison
BC-8	90°	3	3.1	4.2	
BC-9	0°	2	2.9	4.1	
BC-10	0°	3	2.7	3.9	

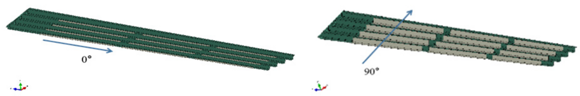

(1) 0°　　(2) 90°

Figure 1. Pasting angle of CFRP strip

III. FINITE ELEMENT MODELING

A. Component unit and material propriety relationship

1) Concrete

The concrete plastic damage model (CDP) in ABAQUS was adopted in this thesis, with the concrete unit of the high accuracy 3D eight-node hexahedral C3D8R solid unit, the constitutive relation was taken from the uniaxial compressive stress-strain relationship curve presented in the Chinese code GB50010 Code for Design of Concrete Structure [22], as follows:

$$y=\begin{cases}\alpha_a x+(3\text{-}2\alpha_a)x^2+(\alpha_a\text{-}2)x^3 & 0\le x\le 1\\ \dfrac{x}{\alpha_d(x-1)^2+x} & x\ge 1\end{cases} \tag{1}$$

$$y=\frac{\sigma}{f_c},\quad x=\frac{\varepsilon}{\varepsilon_c} \tag{2}$$

Where f_c、ε_c were the concrete ultimate compressive stress and strain, respectively, and α_a 、α_d were the parameters of the ascending and descending sections in the constitutive relation curves, respectively, taken according to the specification [23].

2) Steel

T3D2 truss unit was used to simulate the steel reinforcement unit, and the steel constitutive relation was modeled with the bifold ideal plasticity model [23-24] (as shown in Fig.2), i.e., ideal elasticity before yielding, and the hardening stiffness was 0.01 of the steel elasticity modulus from material yielding to reaching the ultimate strength.

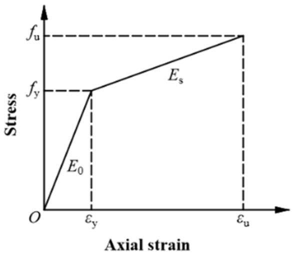

Figure 2. Schematic diagram of steel bar constitutive relationship

Where f_y、ε_y were the yield stress and yield strain, respectively, f_u、ε_u were the ultimate stress and ultimate strain, respectively; E0 was the modulus of elasticity, taken as 200 GPa in this thesis. and Es was the hardened stiffness, Es=0.01E0。

3) CFRP

Since CFRP was an anisotropic material, the Hashin damage was often adopted to describe the damage evolution of fibrous materials in ABAQUS finite element analysis [25-26], which included four independent damage modes, expressed as below.

$$F_f^t = \left(\frac{\bar{\sigma}_{11}}{X^T}\right)^2 + \alpha\left(\frac{\bar{\tau}_{21}}{S^L}\right)^2 - 1 \le 0\text{ ，} \bar{\sigma}_{11} \ge 0 \tag{3}$$

$$F_f^c = \left(\frac{\bar{\sigma}_{11}}{X^C}\right)^2 - 1 \le 0\text{ ，} \bar{\sigma}_{11} \le 0 \tag{4}$$

$$F_m^t = \left(\frac{\bar{\sigma}_{22}}{Y^T}\right)^2 + \left(\frac{\bar{\tau}_{12}}{S^L}\right)^2 - 1 \le 0\text{，} \bar{\sigma}_{22} \ge 0 \tag{5}$$

$$F_m^c = \left(\frac{\bar{\sigma}_{22}}{2S^L}\right)^2 + \left[\left(\frac{Y^C}{2S^L}\right)^2 - 1\right]\frac{\bar{\sigma}_{22}}{Y^C} + \left(\frac{\bar{\tau}_{12}}{S^L}\right)^2 - 1 \le 0\text{，} \bar{\sigma}_{22} \le 0 \tag{6}$$

Where $\bar{\sigma}_{11}$、$\bar{\sigma}_{22}$、$\bar{\tau}_{12}$ were the stress components, XT、XC were the tensile strength and compressive strength in the fiber length direction, respectively, YT、YC were the tensile strength and compressive strength in the fiber vertical direction, SL was the shear strength. In this thesis, the CFRP constitutive relation parameters were taken from literature [27], as shown in Table

Table 2: CFRP material properties

Elastic (single layer board)						Hashin damagemodel					
Elastic Modulus /GPa		Poisson's ratio	Shear modulus /GPa			Longitudinal tensile strength /MPa	Longitudinal compressive strength /MPa	Transverse tensile strength /MPa	Transverse compressive strength /MPa	Longitudinal shear strength /MPa	Transverse shear strength /MPa
E_1	E_2	υ_{12}	G_{12}	G_{13}	G_{23}	X^T	X^C	Y^T	Y^C	S_{12}	S_{13}
211.49	7.93	0.35	5.3	5.3	4	2142.48	1414	37	169	134	120

4) Interaction

The reinforcement was embedded in the concrete through "embed" for simplification and convergence. The bridge and pier models were connected with the hard contact in the normal direction, while the tangential direction was simulated by the friction model with penalty function method, allowing elastic slip deformation, where the friction coefficient was taken as 0.8 according to experience to achieve better simulation effect of the non-integral casting contact between bridge and pier. And the CFRP was glued to the bottom surface of the concrete box girder using "binding" constraints.

B. Boundary conditions and loads

The abutment base was constrained to translate and rotate in three directions to simulate the consolidation in the actual project. And the uniform load was applied to the bridge deck to simulate vehicle loads and pedestrian loads. The completed model building diagram was shown in Fig.3.

Figure 3. Modeling completion diagram

IV. ANALYSIS OF CALCULATION RESULTS

A. Stress clouds

Fig.4 showed a partial stress cloud (the deformation factor was set to 1000 for observation). The following points were obtained by classifying the different variation parameters.

First, the stress clouds under each reinforcement conditions were similar, and the maximum stresses before and after reinforcement appeared in the middle of the span on both sides and the supports, resulting from the arch effect of the continuous beam.

Second，the CFRP stress clouds showed that the CFRP was under tension when the bridge was subjected to traffic loads. Comparing Fig.4(1) and Fig.(2), a larger stress produced from longitudinal CFRP pasting, indicating that the longitudinal pasted CFRP mitigated the bridge stress distribution better than that of CFRP transverse pasting.

Third，comparing Fig. 4(2), Fig. 4(4) and Fig. 4(5), Fig. 4(3), Fig. 4(6) and Fig. 4(7), we found that increasing number of CFRP layers resulted in greater CFRP stresses, indicating that the more layers of CFRP contributed a larger percentage of the structure when under load.

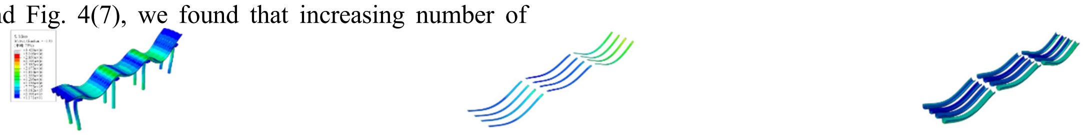

(1) Bridge　　(2) CFRP (0°)　　(3) CFRP (90°)

Figure 4. Stress nephogram

B. *Damage clouds*

Fig.5 showed the comparison of part of the tensile damage clouds (the deformation factor was set to 1000 for observation) Since the displacement clouds were similar for each reinforcement condition, only the comparison of damage clouds for unreinforced bridge B-1, longitudinally reinforced BC-1 (0°) and transversely reinforced BC-5 (90°) were given.

Fig.5 depicted that after reinforcement, the concrete damage area at the beam bottom became larger, indicating that CFRP reinforcement was fully effective.

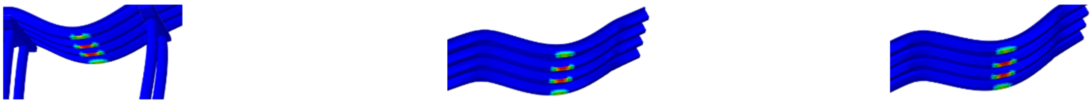

(1) B-1　　(2) BC-1 (0°)　　(3) BC-5 (90°)

Figure 5. Tensile damage nephogram

C. *Transformation clouds*

Fig.6 depicted the partial displacement cloud comparison (the deformation coefficient was set to 1000 for observation). Since the displacement clouds were similar under each reinforcement condition, only the displacement clouds of unreinforced bridge B-1, longitudinally reinforced BC-1 (0°) and transversely reinforced BC-5 (90°) were given for comparison. The deformation clouds were similar for each reinforcement condition, and the maximum deflection appeared in the region of maximum bending moment in the span.

(1) B-1　　(2) BC-1 (0°)　　(3) BC-5 (90°)

Figure 6. Deformation nephogram

D. *The influence of CFRP adhesion direction*

The effects of different CFRP adhesion angles on the maximum stress, maximum deflection, relative cracking load and relative flexural stiffness in the span were given in Fig. 7-Fig. 10. Conclusions that the pasting of CFRP effectively mitigated the stress and deflection of the bridge structure and enhanced the cracking load could be drawn. Compared with the unlaminated bridge B-1, the maximum stresses at the CFRP adhesion angles of 0° to 90° and 0°+90° were reduced by 8.8%, 8.8%, 5.8%, 5.8%, 2.9% and 17.6%, respectively; the mid-span deflections were reduced by 6.5%, 6.5%, 6.5%, 4.3%, 2.1% and 17.4%, respectively; the relative cracking loads were increased by 3.1%, 2.2%, 1.5%, 1.0%, 0.5%, and 3.5%, respectively; and relative flexural stiffness increased by 5.1%, 2.8%, 2.6%, 2.1%, 1.1%, and 5.3%, respectively. In conclusion, the reinforcement efficiency gradually decreased with increasing reinforcement angle, where the best reinforcement effect was 0°+90°

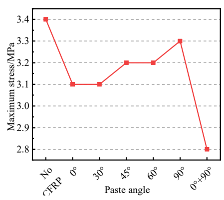

Figure 7 Comparison of maximum stress in different CFRP strip pasting directions

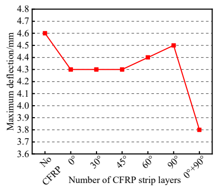

Figure 8 Comparison of maximum deflection in different CFRP strip pasting directions

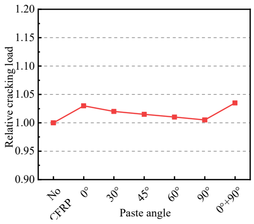

Figure 9 Comparison of relative cracking load in different CFRP strip pasting directions

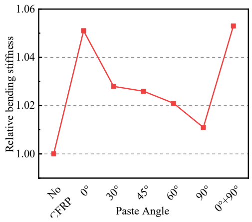

Figure 10 Comparison of relative bending stiffness in different CFRP strip pasting direction

E. Effect of the layer CFRP pasting number

The comparisons of maximum stress, maximum deflection and cracking load in span for different CFRP pasting layers was given in Fig.11-Fig.14.The pictures demonstrated that as the thickness of CFRP increased, the stress and deflection of the bridge structure then decreased and the cracking load gradually increased. Compared with the unlaminated bridge B-1, the maximum stresses were reduced by 8.9%, 14.8% and 20.6% for 1, 2 and 3 layers of longitudinally applied CFRP, respectively; the mid-span deflections were reduced by 6.6%, 10.9% and 15.3%, respectively; the cracking loads were increased by 3.5%, 4.1% and 4.8%, respectively; and the relative flexural stiffness was increased by 5.1%, 5.3% and 6.4%. The maximum stresses of transverse CFRP with 1, 2 and 3 layers were reduced by 3.1%, 5.9% and 8.9%, respectively; the mid-span deflections were reduced by 2.2%, 4.4% and 8.7, respectively; the relative cracking loads were not significantly increased, which was due to the inability of the structural form of CFRP to bear the transverse forces; and the relative flexural stiffnesses were increased by 1.1%, 1.6% and 1.8%, respectively.

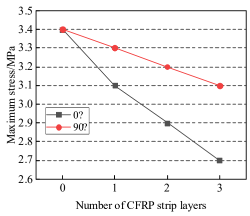

Figure 11 Comparison of maximum stress in different CFRP strip pasting layers

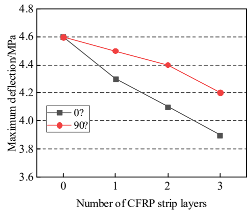

Figure 12 Comparison of maximum deflection in different CFRP strip pasting layers

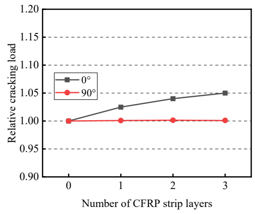

Figure 13 Comparison of relative cracking load in different CFRP strip pasting layers

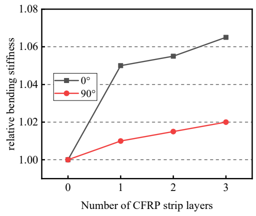

Figure 14 Comparison of relative bending stiffness in different CFRP strip pasting layers

V. CONCLUSION

Through the finite element modeling analysis of 10 reinforcement methods for the bridge in service, the following conclusions were obtained

(1) The applied CFRP reduced the stress and mid-span deflection of the bridge, improved the cracking load and flexural stiffness, and achieved satisfied reinforcement effects.

(2) The stress and displacement clouds of the bridge before and after strengthening were basically similar, with the maximum stress appearing in the bridge compression zone of the box girder in contact with the piers, and the maximum deflection appearing in the span with the largest bending moment.

(3) With the increase of CFRP pasting angle, the reinforcement effect gradually became worse, among which the best reinforcement effect was the pasting angle of 0°+90°, which reduced 17.6% of maximum stress and 17.3% of mid-span deflection, and improved 3.5% of relative cracking load and 5.3 of relative flexural stiffness.

(4) The increase of CFRP layer number lead to the reduction in bridge stress and mid-span deflection, while the cracking load and flexural stiffness were increased to varying degrees.

ACKNOWLEDGEMENT

First of all, I am very grateful to Prof. Oral Buyukozturk for his help in this research. He provided me with scientific ideas and suggestions, and taught me a lot about civil and structural aspects in class, which enabled me to combine civil engineering

with my major (traffic engineering) and laid the theoretical and experimental foundation for this thesis.

Secondly, I would also like to thank my teaching assistant, Xiangyong Duanmu, for his help in simulation experiments and thesis writing. He taught me the basic operation of the finite element software ABAQUS in class and recommended a lot of video operation materials for me to study, and he helped me finish this research paper by providing writing guidance during the writing process.

REFERENCES

[1] Guo DJ, Liang JX, Zhang JQ. Application of Bridge Strengthening Technology [J]. Journal of Highway and Transportation Research and Development, 2004(8): 71 - 73.

[2] Teng JG, Chen JF, Smith ST, Lam L. FRP strengthened RC structures. Chichester: Wiley-Blackwell; 2002.

[3] Hollaway LC, Teng JG. Strengthening and rehabilitation of civil infrastructures using fibre-reinforced polymer (FRP) composites. Elsevier; 2008.

[4] Teng JG, Yuan H, Chen J F. FRP-to-concrete interfaces between two adjacent cracks: Theoretical model for debonding failure[J]. International Journal of Solids and Structures, 2006, 43(18-19):5750-5778.

[5] Teng JG, Chen JF, Smith ST, Lam L. FRP strengthened RC structures. New York: Wiley; 2001.

[6] Rasheed HA. Strengthening design of reinforced concrete with FRP. CRC Press; 2014.

[7] Hollaway LC. A review of the present and future utilization of FRP composites in the Civil infrastructure with reference to their important in service properties. Constr Build Mater 2010;24(12):2419–45.

[8] Pen, pet papers Dai Dai JG, Bai YL, Teng JG. Behavior and modeling of concrete confinined with FRP composites of large deformability. J Compos Constr 2011;15(6):963-73.

[9] Czarnecki L, Kaproń M, Van Gemert D. Sustainable construction: challenges, contribution of polymers, research arena. Restoration Build Monuments 2013;19(2–3):81-96.

[10] Hawileh RA, Nawaz W, Abdalla JA. Flexural behavior of reinforced concrete beams externally strengthened with Hardwire Steel-Fiber sheets. Constr Build Mater 2018; 172:562-73.

[11] Hawileh RA, Abdalla JA, Naser MZ. Modeling the shear strength of concrete beams reinforced with CFRP bars under unsymmetrical loading. Mech Adv Mater Struct 2018:1-8.

[12] Rasheed H, Abdalla JA, Hawileh R, Al-Tamimi A. Flexural Behavior of Reinforced Concrete Beams Strengthened with Externally Bonded Aluminum Alloy Plates. Eng Struct 2017;147(15):473–85.

[13] Kodur VKR, Naser MZ. Importance factor for design of bridges against fire hazard. Eng Struct 2013; 54:207–20.

[14] Kodur VK, Aziz EM, Naser MZ. Strategies for enhancing fire performance of steel bridges. Eng Struct 2017; 131:446–58.

[15] Naser MZ, Kodur VKR. A probabilistic assessment for classification of bridges against fire hazard. Fire Saf J 2015; 76:65–73.

[16] Abdalla JA, Abu-Obeidah A, Hawileh R, Rasheed H. Shear strengthening of reinforced concrete beams using externally-bonded aluminum alloy plates: An experimental study. Constr Build Mater 2016; 128:24–37.

[17] Hawileh RA, Abu-Obeidah A, Abdalla JA, Al-Tamimi AK. Temperature effect on the mechanical properties of carbon, glass and carbon-glass FRP laminates. Constr Build Mater 2015;75(30):342–8.

[18] Hawileh R, Abdalla JA, Hasan S, Ziyada M, Abu-Obeidah A. Models for predicting elastic modulus and tensile strength of carbon, basalt and hybrid carbon-basalt FRP laminates at elevated temperatures. Constr Build Mater 2016; 114:364–73.

[19] Abdalla JA, Hraib FH, Hawileh RA, Mirghani AM. Experimental investigation of bond-slip behavior of aluminum plates adhesively bonded to concrete. Adhes Sci Technol 2017;3(1):82–99.

[20] Banthia N, Nandakumar N, Boyd A. Sprayed fifiber-reinforfiberymers: From laboratory to a real bridge. Concr Int 2002;24(11):47–52.

[21] Ji G, Li G, Alaywan W. A new fire resistant FRP for externally bonded concrete repair. Constr Build Mater 2013; 42:87–96. Teng JG, Yu T, Fernando D. Strengthening of steel structures with fiber-reinforced polymer composites. J Constr Steel Res 2012; 78:131–43.

[22] GB 50010-2002. Code for design of reinforced concrete structures [S]. Beijing: China Planning Press, 2002

[23] Ji J, Yu D, Jiang L, et al. Numerical Analysis of Axial Compression Performance of Concrete Filled Double Steel Tube Short Columns[J]. IOP Conference Series Materials ence and Engineering, 2018, 439(4):042058.

[24] Pagoulatou,M., Sheehan, T, Dai, X. H., Lam, D. (2014) Finite element analysis on the capacity of circular concrete-filled double-skin steel tubular (CFDST) stub columns. J. Engineering Structures, 72: 102-112.

[25] Hashin Z, Rotem A. A Fatigue Failure Criterion for Fiber Reinforced Materials[J]. Journal of Composite Materials, 1973, 7(4):448-464.

[26] Hashin Z. Failure criteria for unidirectional fiber composites. J Appl Mech 1980;47(2):329–34.

[27] C.Fang, M.S. Mohamed Ali, A.H. Sheikh. Experimental and numerical investigations on concrete filled carbon FRP tube (CFRP-CFFT) columns manufactured with ultra-high-performance fibre reinforced concrete[J]. Composite Structures, Volume 239, 2020, 111982.